Springer

KSME

Journal of Mechanical Science and Technology 24 (6) (2010) 1265~1271
www.springerlink.com/content/1738-494x
DOI 10.1007/s12206-010-0335-2

The effect of change in width on stress distribution along the curved segments of stents †

Kyung Soon Jang, Tae Won Kang, Kee Sung Lee, Chul Kim and Tae-Woo Kim*

School of Mechanical Engineering, Kook Min University, Seoul, Korea

(Manuscript Received August 26, 2009; Revised February 5, 2010; Accepted February 22, 2010)

Abstract

Curved structural members are widely seen in our surroundings, such as railway supports in playgrounds resembling a c-ring structure. The common geometry of the curved member consists of a segment of a circular ring with a uniform width. The curved section is of constant width in most cardiovascular stents. This study focuses on curved strut members whose width changes along the curved segment. The location of the maximum equivalent stress varies depending on the manner in which the width changes. When the width is constant or larger toward the top, the maximum equivalent stress is developed at the top. Meanwhile, when the area is reduced toward the bottom, the largest equivalent stress is developed some distance from the top. Simple equations, based on the mechanics of materials and the theory of elasticity, were compared favorably with the results from finite element analysis. Included are elaborations of the distribution of the change of stress. The suggested strategy of changing the width, with refinements, could be applied to the optimal design of structural members, including pipes and medical devices such as stents.

Keywords: Beam; Finite element analysis; Optimal design; Stress

1. Introduction

In designing a member in order to increase the mechanical efficiency of the component, we explore either the selection of materials [1] or the determination of the geometric shape [2]. At times, materials are pre-selected; thus, the external geometry is left for the designer to determine. Thus, the material-efficient design of a component could be achieved based on the intended function, the design constraints, and the objective sought [3]. The objectives of the optimum design could include reducing maximum stress, controlling stress distribution, and minimizing the use of the material, leading to minimum weight of the component [1-4].

Curved structural members in the form of a pipe or a shell are extensively seen in our surroundings [5-8]. For example, Fig. 1(a) shows a curved member supporting a railway in a playground. The curved member in Fig. 1(b) shows a member with a constant cross-section and a reinforcing plate to prevent failure of the component from excessive loading.

Many other examples resemble the segment of a ring experiencing either a compressive or tensile force. Stents are structures that experience extensive tensile forces. A stent [9] is a medical device transplanted into a human coronary artery or an internal organ to expand the narrowed area. They are usually made with ductile metals featuring mesh-like connections. A common geometry for cylindrical stents consists of curved portions [10]. The curved segment is pulled in the direction of the hoop through a straightening action, enabling extensive radial expansion [11]. The cylindrical stent, which is expanded in both radial and hoop (i.e., circumferential) directions, widens the blocked area to the desired extent and avoid collapse by remaining propped up.

When the material for the curved member is pre-determined, only the geometric design could be altered to ensure lifetime durability [12] and accomplish optimum design. A common geometry for the curved member consists of a segment of a circular ring with a constant cross-section or uniform width [2, 13-15]. Numerical models and experiments (combined with numerical investigations) on behaviors related to stents have been reported [11, 14-16].

This study investigates the effect of the change of width for the curved strut of a stent, which resembles a curved bow in sports, on the stress distribution along the circumference of the curved length. The curved strut of a stent is part of a cylindrical segment and is slightly warped, as shown in Fig. 2(a). However, in this study, the curved strut member is assumed to lie on a plane to compare the present findings with available analytical estimations. Two independent analytical approaches,

† This paper was recommended for publication in revised form by Associate Editor Tae Hee Lee

*Corresponding author. Tel.: +82 2 910 4678, Fax: +82 2 910 4655
E-mail address: twkim@kookmin.ac.kr

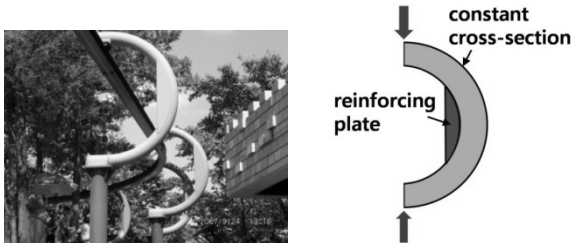

(a) (b)

Fig. 1. (a) Railway support featuring a curved member; (b) Schematic of a curved member and a reinforcing plate under compression.

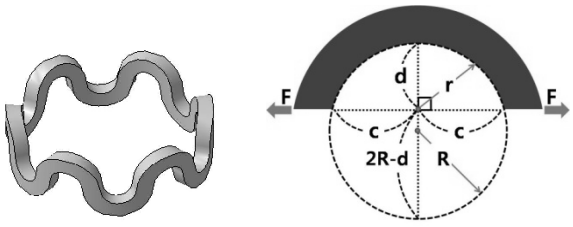

(a) (b)

Fig. 2. (a) The typical segment in a cardiovascular stent featuring a curved part; (b) A circular arc experiencing tensile forces at the end-points.

based on the mechanics of materials [2] and the theory of elasticity [17], have been undertaken. The first approach in computing the stress in a curved flexural member considers force and moment equilibrium, and the equation based on the theory of elasticity is generated from the postulated stress function. The results from subsequent finite element analysis (FEA) were then compared with the analytical estimations of the stress distribution. This paper discusses findings on the variation of the stress distributions with the relative position within the curved member.

2. Methods

2.1 The approach using the mechanics of materials

One approach in determining stress distribution for a curved flexural member is based on the mechanics of materials. Unlike straight beams, the neutral and centroidal axes of a curved member are not coincident [2]. When the curvature is large, the stress does not vary linearly from the neutral axis. Therefore, the elementary bending-stress formula, determined by dividing the moment by the sectional modulus, gives an inaccurate estimation of the resultant stress. The worked-out examples found in textbooks [2, 13] mostly deal with a hook with curves bounded by two concentric circular arcs. For a circular arc with a radius of R as shown in Fig. 2, the geometric relation is shown in Eq. (1).

$$c^2 = d(2R - d) \tag{1}$$

A typical curved segment could be modeled with a surface bounded by two straight lines and two curved circular arcs. It

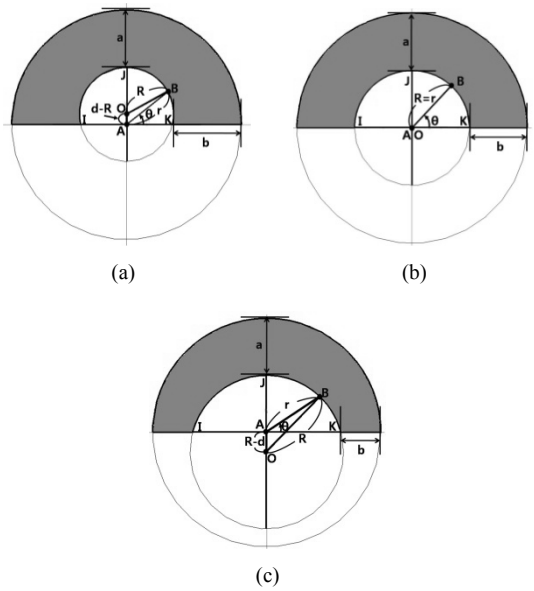

(a) (b)

(c)

Fig. 3. Curved members bounded by two circular arcs with a relative width: (a) greater than unity; (b) equal to unity and (c) smaller than unity.

is natural that the centers of the two concentric circular arcs coincide. The distance from the center to any point on the arc remains constant, as shown in Fig. 3(b). If the width of the curved member is not constant along the curved segment, the distance would no longer be constant and would depend on the relative location on the arc. Therefore, for members with non-uniform widths, the distance from the center to a point on the arc has to be determined as an independent function of the angle of the arc.

The present study defined the relative width in order to determine systematically the effect of the relative width on the stress distribution. The relative width refers to the ratio of the two widths at the end locations, as shown in Figs. 3(a) to 3(c). Two concentric, circular arcs with two different constant radii could result in identical widths, a and b, leading to a relative width of one. Meanwhile, the relative width could be larger or smaller than unity depending on the widths, as shown in Fig. 3 (a) or 3(c). Several relative widths, which were either greater or smaller than unity, were modeled and analyzed.

The geometric modification of the cell with different relative widths was obtained using the procedure described below.

The radius of the outer arc was not changed. In addition, the width-a (in Fig. 3) was not altered; the width-b— which satisfied a certain relative width—was determined. Three points on the same plane (i.e., points I, J, and K in Fig. 3) enabled a unique determination of the inner circular arc. Two straight lines were added to complete a final curved surface segment.

For a triangle △OAB in Fig. 3(a), the distance (r) from point A to any point on the inner arc was calculated using Cosine-rule [15] as shown in Eq. (2a).

$$R^2 = r^2 + (d - R)^2 - 2(d - R)r \cdot \cos(\frac{\pi}{2} - \theta) \tag{2a}$$

A similar relation was obtained for triangle △OAB in Fig. 3(c).

$$R^2 = r^2 + (R-d)^2 - 2(R-d)r \cdot \cos(\frac{\pi}{2} + \theta) \quad (2b)$$

Both Eqs. (2a) and (2b) can be simplified to Eq. (2c).

$$R^2 = r^2 + (R-d)^2 + 2(R-d)r \cdot \sin\theta \quad (2c)$$

The radius of the circle (i.e., R in Fig. 2), was eliminated using the relationship shown in Eq. (1). The combination of Eqs. (1) and (2c) and the solution of the quadratic equation for the distance, *r*, yielded Eq. (3) below.

$$r = \frac{(d^2 - c^2)}{2d}\sin\theta + \sqrt{\left(\frac{d^2 - c^2}{2d}\sin\theta\right)^2 + c^2} \quad (3)$$

Eq. (3) satisfied two boundary conditions at two end-points, where the distance, *r*, was equal to *c*(at $\theta = 0$) or *d* (at $\theta = \frac{\pi}{2}$) (Fig. 2). Since the two distances (*c* and *d* in Fig. 2) became identical for a member shown in Fig. 3(b), Eq. (3) implies that the distance, *r*, equals the radius of the circle, which is *R* in Fig. 2. The inner arc was chosen because it experienced tensile hoop stresses leading to potential failure in the surface-crack opening mode [2]. By substituting Eq. (3) into Eq. (4), the hoop (or circumferential) stress at any point along the inner arc was obtained. The total hoop stress was determined by adding the extensional and flexural stress components [2], as shown below.

$$\sigma = \frac{F}{A} + \frac{M}{A} \cdot \frac{(r_n - r)}{(r_c - r_n)r} \quad (4)$$

In Eq. (4), *A* is the cross-sectional area, *F* is the force component acting on the cross-section, and *M* is the bending moment computed in the centroidal axis. The second term in Eq. (4)—the flexural stress component—is a product of the moment over the area and a geometrical multiplier determined by the relevant distances. Since the neutral and centroidal axes are not coincident [2], we determined the distances from point A in Fig. 3 to the neural and centroidal axes as r_n and, r_c, respectively. The explanations regarding the use of Eq. (4) are presented in [2, 13].

2.2 The elasticity approach

Another analytical expression to compute for stress at a point is based on the theory of elasticity. The theory is derived from the stress function [16, 19-20]. Cutting an annulus of constant width produces a curved member, as shown in Fig. 3(b). The formula to determine the hoop stress for a member with uniform width could be found in [14]. The formula uses two constant inner and outer radii. The geometries shown in Fig. 3 are different from one another in that only the inner radius is a function of the angle, as explained in Eq. (3). Consequently, a simple approximation was made by replacing the constant inner radius with a radius which changed with the angle of the arc, as shown in Eqs. (5a) and (5b). The angle in Eq. (5a) was defined in a counter-clockwise direction from the bottom (i.e., point K in Fig. 3) toward the top (i.e., point J in Fig. 3). The outer radius (*b*) remained constant, as described in Section 2.1. The force (*F*) was then applied in the direction shown in Fig. 2.

$$\sigma = \frac{F}{N}\left[-3r + \frac{r^2 b^2}{r^3} + \frac{(r^2 + b^2)}{r}\right] \cdot \sin\theta \quad (5a)$$

$$N = (r^2 - b^2) + (r^2 + b^2)\ln\frac{b}{r} \quad (5b)$$

2.3 FEA

The curved member was modeled and analyzed using the ABAQUS FEA program [21]. Prior to actual computations for the geometries under study, the FEA modeling technique was checked for the crane hook illustrated in reference [2]. The curved surface segment was bounded by two concentric circular arcs, implying that the width was constant along the curved segment. The stresses obtained through FEA were compared with analytical answers in reference [2]. The computed values obtained through Eq. (5a), based on the theory of elasticity, were slightly greater than those found in [2], based on the mechanics of materials. The FEA results were less by about 10% than the estimations from the two theories.

Similar computations were conducted for the curved surface, in which the width changed along the curved segment. A Young's modulus of 190 GPa and a Poisson's ratio of 0.3, otherwise known as the elastic properties of stainless steel 316L, were used while performing the computations. Stainless steel 316L was chosen because many cardiovascular stents used the material [22]. However, neither Eq. (4) nor (5a) was affected by the Young's modulus of the member. After conducting FEA, it was found that a change in the Young's modulus did not cause any significant change in the resultant stress.

In this study, FEA results were based on computations of a curved member with a square cross-section. The square cross-section was adopted because the common cross-section of stents was found to be closer to a square than a circle. The stresses were taken from the nodal points along the mid-plane at the cross-section. Continuum, eight-noded, block elements were used for each analysis. Four different relative widths were selected for modeling, with ratios of 1.2, 1.0, 0.7 and 0.3, respectively.

3. Results and discussion

Fig. 4 shows that hoop stresses obtained from two analytical approaches and FEA agree reasonably well with one another. Due to the symmetry in Fig. 3, we can observe stresses along

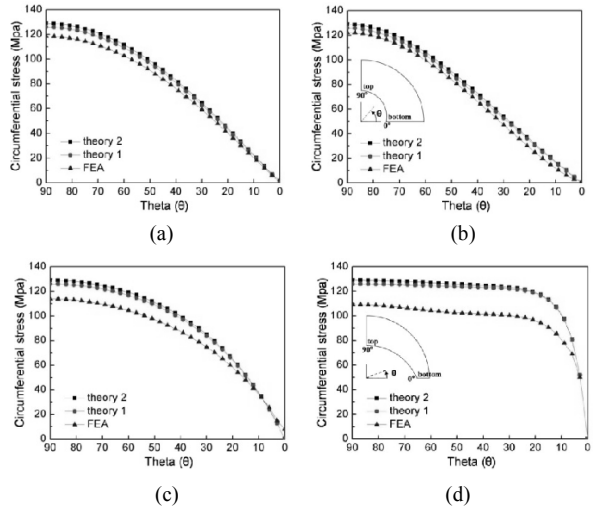

Fig. 4. Hoop stresses from two analytical estimations and results from FEA for a relative width of: (a) 1.2; (b) 1.0; (c) 0.7 and (d) 0.3.

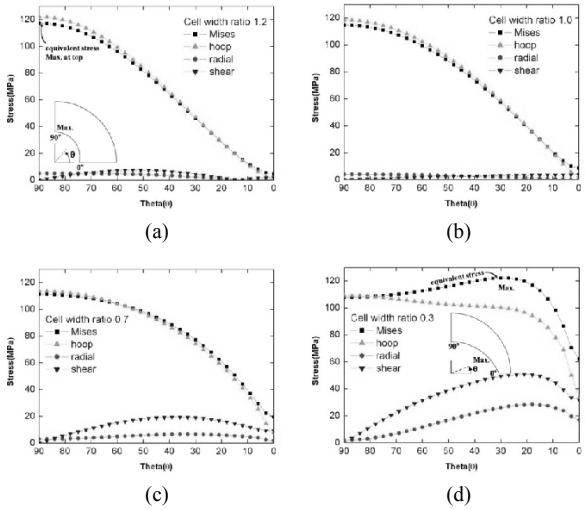

Fig. 5. FEA results on the equivalent and individual stress components for relative widths of: (a) 1.2; (b) 1.0; (c) 0.7 and (d) 0.3.

the inner arc in the right half of the model. The angles starting from 0 to 90° correspond to the direction from points k to j in Fig. 3. As the counter-clockwise angle have been assumed positive in Fig. 3, the numbers in the abscissa are shown in descending order for easier visual understanding. "Theory-1" in Fig. 4 refers to approximations by the mechanics of materials, and "theory-2" represents the results based on the theory of elasticity. Figs. 4(a) and 4(b) show that hoop stress increases with the angle, starting from zero, and reaches the maximum at the top where the angle (θ) is 90°. The maximum hoop stress occurs at the top mainly because the bending moment is largest at the top owing to the longest moment arm. This part of the explanations will be detailed in later sections. An examination of Figs. 4(a) to 4(d) reveals that the maximum hoop stress at the top, as obtained through FEA, decreases slightly as the relative width decreases.

The hoop stresses between 20 and 80° tend to increase as the relative width decreases from 1.0 to 0.3, as shown in Figs. 4(b) to 4(d). When the relative width becomes 0.3, the curve for the hoop stress between 20 and 80° shows a fairly flat region, as shown in Fig. 4(d).

Assuming that the failure of ductile metal is governed by the distortion-energy theory [2], each component of the stress and the equivalent (or Mises) stress are compared in Fig. 5. In Figs. 5(a) and 5(b), the radial and shear stresses are relatively negligible compared with the large hoop-stress component. However, Figs. 5(c) and 5(d) show that the radial and shear stresses increased because the decreased relative width—implying a smaller cross-sectional area toward the bottom—resulted in increases in the radial and shear stresses in those regions.

Combining all stress components to compute the equivalent stress for each case indicates that the equivalent stress varies with the angle of the arc. When the relative width is equal to or greater than unity, the largest equivalent stress occurs at the top where the angle of the arc is 90°. Meanwhile, as the relative width for the cell decreases, the largest equivalent stress is found some distance from the top. The angle of the arc for the largest equivalent stress is roughly 30°, as shown in Fig. 5(d). The development of the maximum equivalent stress at the region away from the top for a curved member with a smaller relative width is caused by a combination of the two following reasons. Primarily, the hoop stress tends to become nearly insensitive to the angle and fairly flat as the relative width becomes smaller than one. Second, the radial and shear stresses tend to increase due to the reduced cross-sectional area as the relative width decreases.

Fig. 6 shows a typical hoop-stress contour obtained through FEA for the model shown in Fig. 3(b). The contours are drawn in the cylindrical-coordinate system to represent the change in the stress with the angle of the arc. The forces at two locations tend to straighten the curved portion, leading to tensile and compressive stress along the inner and outer arcs, respectively. The results are consistent with the analytical expectation [2, 13], demonstrating the validity of the FEA modeling technique.

Comparing equivalent stress contours indicates different potential failure sites for curved members with different relative widths. Figs. 5(d) and 7(b) show that the maximum equivalent stress contour for the relative width of 0.3 is found between 20 and 50° with regard to the angle of the arc. The curved member with a relative width either equal to or greater than unity shows the largest equivalent stress at the top region, as shown in Fig. 7(a).

The hoop-stress component contributes most significantly in determining the equivalent stress for the curved member, as illustrated in Fig. 5. The total hoop stress could be broken into two contributing terms, namely, the extensional and flexural stress components, as shown in Eq. (4). The extensional component is much smaller than the flexural stress (Fig. 8). This is true regardless of the relative widths.

To examine the sensitivity of each extensional and flexural

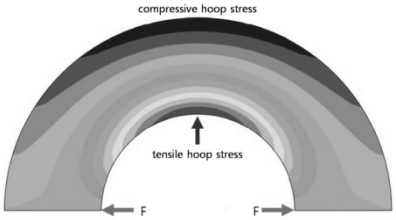

Fig. 6. A typical FEA contour showing regions for tensile and compressive hoop stresses.

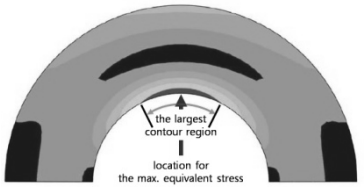

(a)

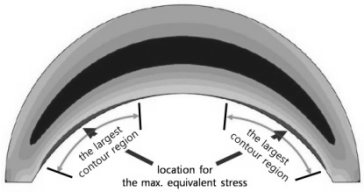

(b)

Fig. 7. The largest stress that: (a) develops at the top and (b) develops not at the top, but in the neighborhood of the top region.

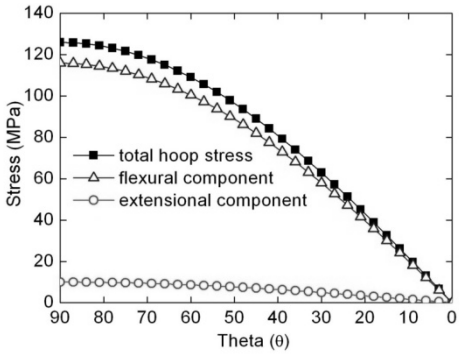

Fig. 8. The change in the total hoop stress and in each stress component.

stress component to the angle of the arc and the relative width, each stress component was normalized with respect to the largest magnitude of each variable. When the relative width is greater than or equal to unity, both extensional and flexural components increase with the angle similar to those shown in Figs. 9(a) and 9(b). As the relative width decreases to 0.3, the flexural component is nearly insensitive; and an almost plateau value is found at angles greater than 20°. This implies that the flexural component of the hoop stress is the primary factor causing a fairly flat curve, as shown in Fig. 4.

As relative widths change, the moment divided by the cross-sectional area changes with the angle of the arc. Another factor influencing the stress distribution is the change of each distance from the center to the neutral and centroidal axes, as

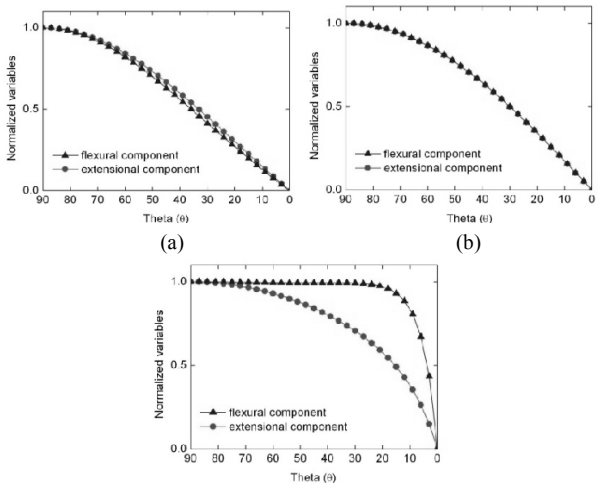

(a) (b)

(c)

Fig. 9. Normalized extensional and flexural stress components at relative widths of: (a) 1.2; (b) 1.0 and (c) 0.3.

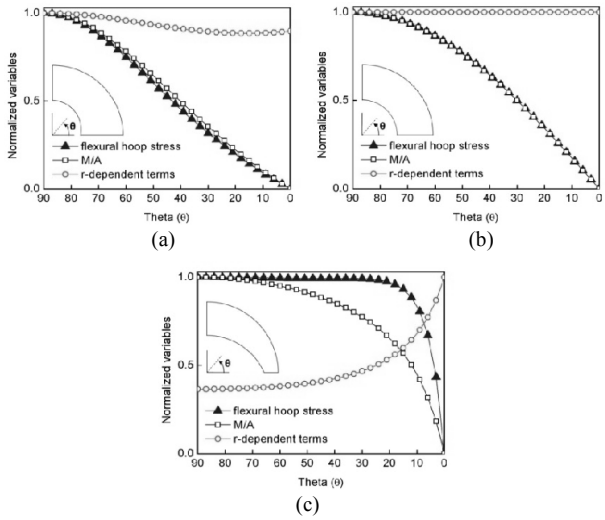

(a) (b)

(c)

Fig. 10. Variation of the flexural stress, moment over the cross-sectional area, and the geometrical variables determined by distances for the cell with relative widths of: (a) 1.5; (b) 1.0 and (c) 0.3.

described in Eq. (4). For the member with a relative width of 1.5, the moment divided by the cross-sectional area determines the flexural stress. The effect of the multiplier, which is determined by the relevant distances, is marginal, as shown in Fig. 10(a). Since the cross-sectional area remains constant for a relative width of unity, the multiplier depending on the relevant distances does not affect the flexural stress, as shown in Fig. 10(b). However, for a cell with a relative width of 0.3, the decrease in the flexural stress is nearly compensated by the increase of the factors depending on the distances, as shown in the open symbols of Fig. 10(c). Therefore, the multiplication of the flexural stress and a factor depending on the distances results in a fairly flat graph between 20 and 80°, as shown in Fig. 10(c). These findings, together with the results shown in Fig. 5, clearly explain why the maximum equivalent stress is developed at a different location depending

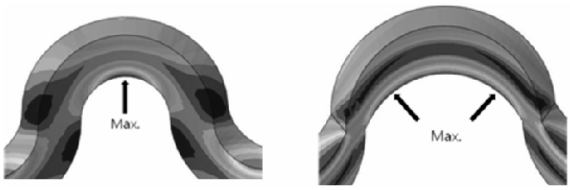

(a) (b)

Fig. 11. Comparison of contours showing different locations for maximum Mises stress within the modeled stent with relative ratio (a) of unity and (b) less than unity.

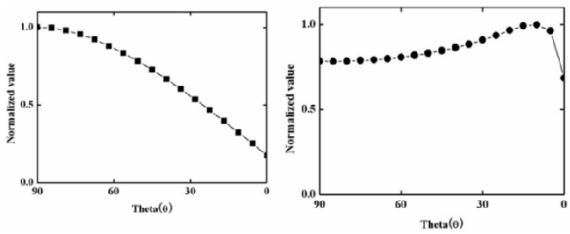

(a) (b)

Fig. 12. Variation of Mises stress along the curved stent segment showing different locations for maximum Mises stress.

on the relative width.

The results in Fig. 7 are based on the curved member lying in a plane, whereas the actual curved stent strut member is slightly warped in the circumferential direction as shown in Fig. 2(a). Solid block finite elements found in the ABAQUS program were used to model the curved stent strut member. The curved segments were modeled with uniform relative width and changing relative width. The obtained stress contours are shown in Fig. 11. Figs. 7(a), 11(a), and 12(a) all show that the maximum of the equivalent stress is found at the top of the curved segment with uniform relative width. However, as shown in Figs. 7(b) and 11(b), the curved members with the relative value less than unity exhibit the location for maximum equivalent stress at certain distance away from the top of the segment. This is because the gradual change of the cross-section within the curved segment plays a significant role in changing the stress distribution. The variation of equivalent stress (i.e., Mises stress) along the curved stent segment, as shown in Fig. 12(b), clearly indicates that the maximum stress for the curved member with the relative width less than unity does not occur at the top.

The present study focuses on a curved member, in which the width changes along the curved segment. The location of the maximum equivalent stress varies, depending on the way the cross-sectional area changes. When the area reduces toward the bottom, the largest equivalent stress develops at some distance from the top. Simple equations, based on the mechanics of materials and elasticity, compared favorably with FEA. In designing a curved member, as shown in Fig. 1(a), an extra reinforcing plate could avoid premature failure resulting from excessive loading. The gradual change in the width along the curved segment could also influence the stress distribution and the maximum equivalent stress, which may help reduce the incidence of failure.

In this work, the proposed design strategy of changing the relative width along the curved segment may be used to elaborate results for many other curved members, including medical devices such as stents. The present study validates the fundamental concept that the curve could be optimized depending on design constraints [4].

4. Conclusions

This study focuses on a curved member in which the width changes along the curved segment. The location of the maximum equivalent stress varies depending on the way the cross-sectional area changes. When the area reduces toward the bottom, the largest equivalent stress develops at some distance from the top. This change of location for the largest stress is the primary reason why: (1) the cross-sectional area reduces, leading to increased radial- and shear-stress components, and (2) the value of the flexural hoop stress tends to become insensitive to the location.

The estimations of the stress based on the mechanics of materials and the theory of elasticity accounted well for the change in the location of the maximum equivalent stress. The results obtained through FEA agree well with the analytical estimations. The current methods and findings may be used to design or elaborate results for other curved members, such as those found in cardiovascular stents.

Acknowledgment

This work was supported by the KookMin University Research Program 2010 in Korea. One of authors (T. Kang) was supported by the Korea Research Foundation Grant (359-2008-1-D00001).

References

[1] M. F. Ashby and D. R. H. Jones, *Engineering Materials*, 3rd Ed. Elsevier, (2005).

[2] J. E. Shigley, C. R. Mischke and R. G. Budynas, *Mechanical Engineering Design*, 7th ed. McGrawHill, 2003, 155-156.

[3] M. F. Ashby, *Materials Selection in Mechanical Design*. 3rd Ed. Elsevier, (2005).

[4] J. S. Arora, *Introduction to optimum design*, 2nd Ed. Elsevier, (2004).

[5] B. Y. Kim, C. Kim, S. G. Song, H. G. Beom and C. Cho, A finite thin circular beam element for out-of-plane vibration analysis of curved beams, *Journal of Mechanical Science and Technology*, 23 (2009) 1396-1405.

[6] N. Kim and D. K. Shin, A series solution for spatially coupled deflection analysis of thin-walled Timoshenko curved beam with and without elastic foundation, *Journal of Mechanical Science and Technology*, 23 (2009) 475-488.

[7] M. T. Piovan and V. H. Cortinez. Linear viscoelastic analysis of straight and curved thin-walled laminated composite

beams. *International Journal of Solids and Structures*, (2008) 45, 15, 3466-3493.
[8] M. Altinok, E. Burdurlu and K. Ozkaya, Deformation analysis of curved laminated structural wood elements. *Construction and Building Materials*, 22 (2008) 1643-1647.
[9] A. Colombo, G. Stankovic and J.W. Moses, Selection of coronary stents. *J. of the American College of Cardiology*, (2002), 40,6,1021-1033.
[10] L. Petrini, F. Migliavacca, F. Auricchio and G. Dubini, Numerical investigation of the intravascular coronary stent flexibility. *J. of Biomechanics*, (2004),37,495-501.
[11] F. Migliavacca, L. Petrini, V. Montanari, I. Quagliana, F. Auricchio and G. Dubini, A predictive study of the mechanical behavior of coronary stents by computer modeling. *Medical Engineering and Physics*, (2005),27,13-18.
[12] S. Wiersma and D. Taylor, Fatigue of materials used in microscopic components. *Fatigue & Fracture of Engineering Materials & Structures*, (2005, 28,1153-1160.
[13] R. C. Hibbeler, Mechanics of Materials, (1997), 328-337, Prentice-Hall, 3rd ed.
[14] K. Takashima, T. Kitou, K. Mori and K. Ikeuchi, Simulation and experimental observation of contact conditions between stents and artery models. *Medical Engineering & Physics*, (2007), 29, 326-335.
[15] W. Wu, D. Z. Yang, M. Qi and W. Q. Wang, An FEA method to study flexibility of expanded coronary stents. *J.of Materials Processing Technology*, (2007),184, 447-450.
[16] Y. P. Kathuria, The potential of biocompatible metallic stents and preventing restenosis. *Materials Science and Engineering A*, (2006),417,40-48.
[17] J. R. Barber. *Elasticity*. 2nd. Kluwer Academic Publishers, (2002),126-127.
[18] J. L. Meriam, *Engineering Mechanics*, Statics, Wiley, (1978), 382.
[19] A. K. Mal and S. J. Singh, *Deformation of elastic solid*s, Prentice-hall (1991), 191-210.
[20] R. G. Budynas, *Advanced Strength and Applied Stress Analysis*, McGrawHill, (1999), 2nd, 309.
[21] ABAQUS user's manual, Simulia, (2008).
[22] F. Etave, G. Finet, M. Boivin, J. Boyer, G. Rioufol and G. Thollet, Mechanical properties of coronary stents determined by using finite element analysis *J. of Biomechanics*, (2001), 34, 1065-1075.

Kyung Soon Jang received his Master's degree at the Department of Mechanics and Design at Kook Min University. He is currently working as an engineer at Hyundai Motor Company.

Tae-Woo Kim received his Ph.D. in Engineering Mechanics at the Pennsylvania State University in 1990. He is currently working as a professor at Kook Min University. His interests include mechanical engineering design, mechanics, and mechanical properties of materials.